

Complex investigations of structural and thermal properties of silica-titania adsorbents

J. Skubiszewska-Zięba · B. Charmas ·
R. Leboda · V. A. Tertykh · V. V. Yanishpolskii

ICVMTT2011 Conference Special Chapter

© The Author(s) 2011. This article is published with open access at Springerlink.com

Abstract Mesoporous titanium-containing silicas with different Titania contents were investigated. The structural parameters of the materials were characterized by low-temperature adsorption/desorption of nitrogen and X-ray diffraction analysis. The thermodesorption of water using the quasi-isothermal thermogravimetry as well as the differential scanning calorimetry were used to characterize thermal and surface properties of these materials. The adsorbed water layers and the concentration of weakly and strongly bound water as well as the surface free energy on the adsorbent/water interfaces were calculated. It was stated that the increase of Titania content causes a gradual decrease of specific surface area and formation of biporous structure inside the tested materials. The water thermodesorption from the surface proceeds in two or three stages, which is connected mainly with pore distribution and TiO_2 content. One can observe the increase of the total surface free energy (ΔG_Σ) with the increasing TiO_2 content, but the largest ΔG_Σ value at the adsorbent/strongly bound water interface is exhibited by the adsorbent of intermediate content (30%) of TiO_2 . Freezing temperature of water contained in the pores of the studied materials is connected largely with their porous structure. Due to the well developed porous structure, the water freezing process is a multi-stage one.

Keywords Mesoporous titanosilicas · Porous structure · Q-TG · DSC · Water layers · Surface free energy

Introduction

The rapid development of research on the preparation of ordered mesoporous materials began in the early 1990s [1], when the Mobil Corporation has reported new method of materials designated as M41S synthesis. Such materials are characterized by high specific surface area and well developed porous structure with ordered framework and narrow pore size distribution. The structure of mesoporous materials allows using them as host materials, catalyst for reactions of large molecules [2] and chromatographic materials. They can be modified by incorporation of different metals in the form of elements, ions or oxides which can create or enlarge the activity inside the pores. The incorporation of ions of transition metals into the framework of such materials (especially titanium) gives additional special catalytic properties [3–11].

Silica-titania materials (STM) possessing different compositions and physico-chemical characteristics are widely used as fillers, pigments, catalysts, catalyst supports, etc. [3, 12–14] They also demonstrate photocatalytic and oxidative activity [15, 16]. Mesoporous titania-silica materials can be prepared by three methods [17]: (1) one-pot synthesis (the metal precursor is added directly to a silicon source and metal becomes part of the wall structure) [6, 18], (2) template ion-exchange (the ion template in as-prepared material is exchanged with other metal ions from the solution) [19] as well as (3) post-synthesis modification (numerous Si–OH groups react with the organometallic complex or another source of metal) [20, 21]. It is known that the synthesis techniques used for preparation (sol–gel,

J. Skubiszewska-Zięba · B. Charmas (✉) · R. Leboda
Department of Chromatographic Methods, Faculty of Chemistry,
Maria Curie-Skłodowska University, Maria Curie-Skłodowska
Sq.3, 20-031 Lublin, Poland
e-mail: barbara.charmas@poczta.umcs.lublin.pl

V. A. Tertykh · V. V. Yanishpolskii
Institute of Surface Chemistry, National Academy of Science of
Ukraine, Kiev 252022, Ukraine

Table 1 Structural parameters of silica-titania adsorbents

Sample	TiO ₂ content/ mol %	$S_{\text{BET}}/$ m ² /g	$V_p/$ cm ³ /g	$R_{\text{ave}}/$ nm	$R_{\text{dom}}/$ nm
ST ₁	1	924	0.47	1.0	1.04
ST ₁₅	15	805	0.45	1.1	1.04; 2.13
ST ₃₀	30	702	0.52	1.5	1.14; 2.02
ST ₅₀	50	529	0.59	2.3	1.89
ST ₇₀	70	353	0.45	2.6	2.43

high-temperature hydrolysis, chemical vapor deposition (CVD) strongly affect the structure and properties of STM. Titania-silicas can possess (a) complex structure both in the bulk and at the surface layer, as it is in the fumed ST or (b) separated phases of TiO₂ and SiO₂ with a clear-cut phase boundary when one of these oxides is formed on another, which is a substrate (e.g., using the CVD technique). Naturally, the activity of solids in various adsorption and catalytic processes is affected by many factors, i.e., porous structure, chemical nature of surface functional groups and their natural distribution and concentration [22–24]. The surface and sorption properties of such materials depend strongly on the degree of hydration, i.e., the amount of bound and physically adsorbed water. Many studies suggest that the water contained in pores of such materials changes its physicochemical properties because of interactions with the solid surface [25–27]. Thus, studying the phase transitions of water bound to the surface of such materials we obtain additional information about their porous structure and the nature of the surface.

The aim of this article was to investigate the effect of chemical compositions (SiO₂/TiO₂) and the porosity of a series of silica-titania adsorbents on the structure of adsorbed water layers.

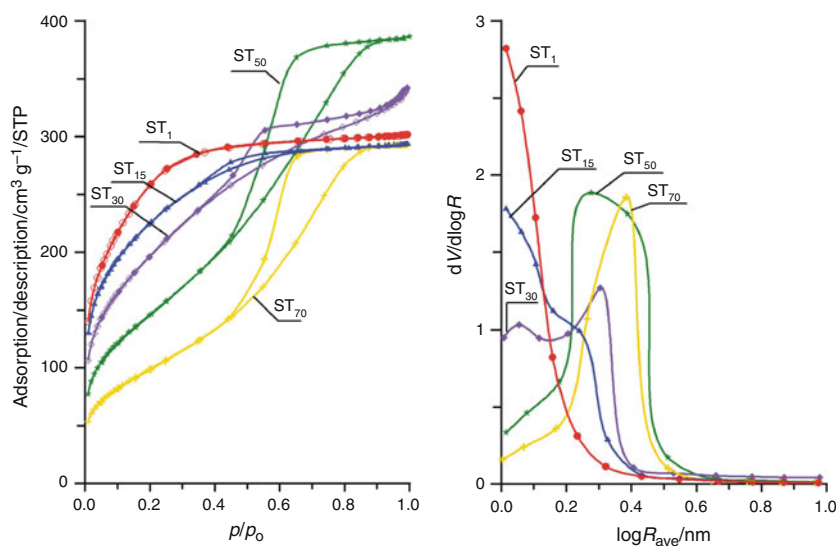
Experimental

Titania-silica samples (containing from 1 to 70 mol % of TiO₂) were prepared by using the templating approach to synthesize mesoporous silica-based molecular sieves partly substituted with titanium-large-pore analogs of titanium silicalite. The reaction of TEOS and Ti(i-OC₃H₇)₄, as SiO₂ and TiO₂ precursors, with octadecyltrimethylammonium chloride (ODTMA) as a template was performed. The ratio of ODTMA: (SiO₂ + TiO₂) was equal to 0.27. The details of the preparation procedure were described in [14].

The characterization of synthesized samples was performed by nitrogen adsorption/desorption isotherms measured at 77 K using the ASAP 2405 Micromeritics apparatus. The specific surface area (S_{BET} , Table 1) was calculated using the BET equation [28] at p/p_0 between 0.06 and 0.2 (where p and p_0 denote the equilibrium and saturation pressure of nitrogen, respectively). The pore volume V_p was determined at $p/p_0 \approx 1$. The average pore radius (R_{ave}) was calculated using a cylindrical pore model $R_p = 2V_p/S_{\text{BET}}$. Pore volume distributions in the function of their radius were calculated according to the Barrett-Joyner-Halenda (BJH) method [29]. On the basis of this dependence the dominant pore radius (R_{dom}) was determined. The X-ray diffraction analysis (XRD) was performed using the automated diffractometer DRON-3M, Cu-K_α radiation.

Thermodesorption of water from the surface of investigated samples was carried out under quasi-isothermal conditions (Q-TG) in the range of 293–573 K using a Derivatograph C (Paulik, Paulik and Erdey, MOM, Hungary). Before the Q-TG measurements the water vapor was adsorbed on the surface of studied samples at room temperature (293 K) for 72 h. Then the weighed portions (about 50 mg) of adsorbents were placed in the special

Fig. 1 Low-temperature adsorption/desorption of nitrogen (a) and pore volume distribution functions in respect to their radius (b) for the silica-titania adsorbents



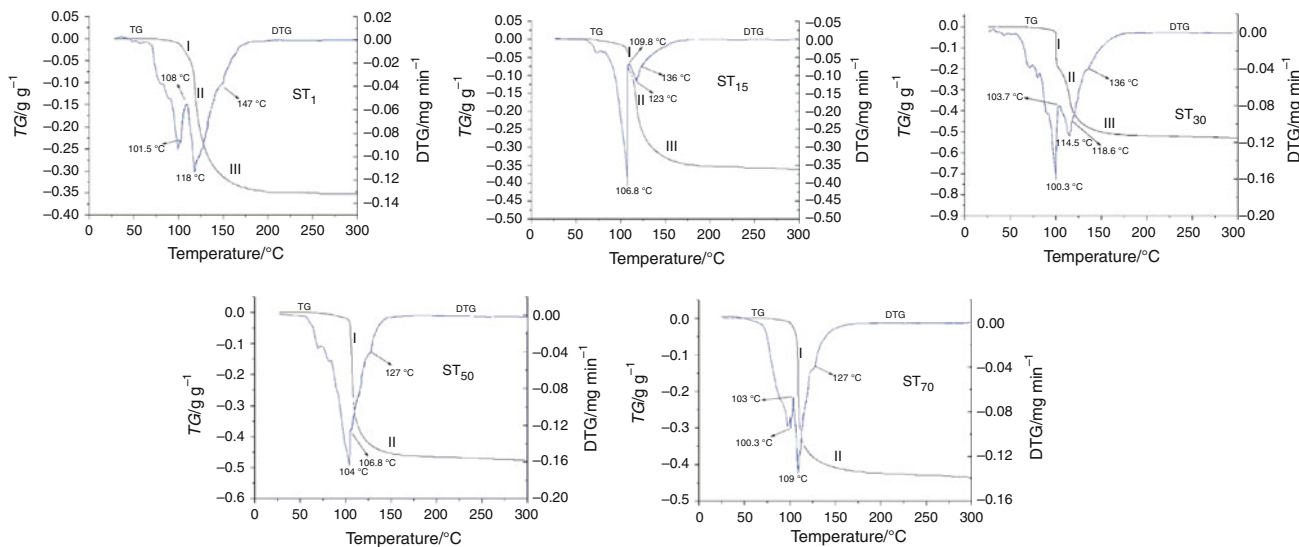


Fig. 2 The Q-TG and Q-DTG curves of water thermodesorption from the tested adsorbents

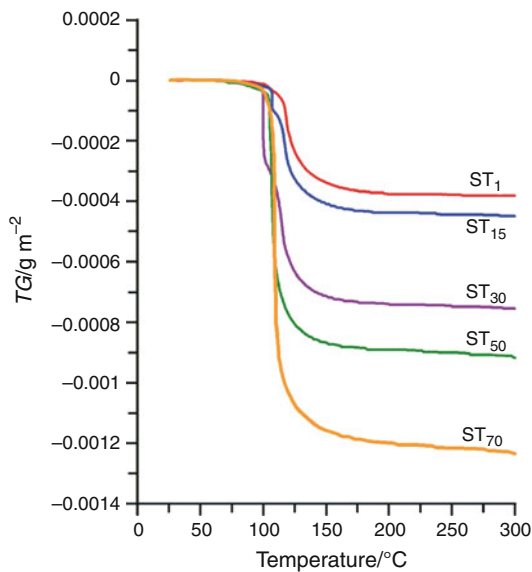


Fig. 3 The course of water mass loss curve as a function of the temperature increase

spherical platinum crucible of the derivatograph. The experimental data of quasi-thermogravimetric measurements correspond to water mass loss in accordance with temperature changes. When measurements are performed over a temperature range without any chemical reactions leading to changes in the sample mass then the $\Delta m = f(T)$ dependence reflects changes in concentration of the substance present on the adsorbent surface under equilibrium. These data were used as initial ones for calculation of energetic characteristics of the tested samples. This method was described precisely in [30, 31]. On the basis of the obtained data, total concentrations of water adsorbed on the

surface of studied adsorbents (mg/g) were calculated. The number of statistical monolayers “ n ” of water was determined from the formula:

$$n = \frac{TG_{max} N_{\omega}}{S_{BET} M} \tag{1}$$

where ω —the surface occupied by one adsorbed water molecule (assumed 0.09 nm^2 , N —the Avogadro number, S_{BET} —the specific surface area of the tested adsorbents (m^2/g), TG_{max} —the maximum mass loss at 573 K (mg/g), M —molar mass of water (18 g/mol).

Thermal properties of the silica-titania adsorbents were performed using Differential Scanning Calorimetry (DSC PYRIS Diamond Perkin Elmer, USA). The DSC method was used to indicate the energetic effects of the interfacial phenomena, which takes place during freezing of strongly and weakly bound water connected with the surface of tested adsorbents.

Results and discussion

Low-temperature adsorption/desorption of nitrogen and pore volume distribution functions in respect to their radius for the silica-titania adsorbents are presented in Fig. 1. As follows from the course of the curves of adsorption–desorption isotherms (Fig. 1a), the smaller is the TiO_2 content in the sample mass, the larger is contribution of micropores. The ST_1 adsorbent is microporous, the adsorption isotherm reaches plateau at higher values of pressure and does not exhibit a hysteresis loop. With the TiO_2 increase in the sample mass, drop in the micropore volume is observed. For the adsorbents ST_{15} and ST_{30} the structure becomes bimodal, i.e., we can observe two peaks corresponding to

Fig. 4 The dependence of water free energy changes on the function of its concentration on the surface of the studied silica-titania adsorbents

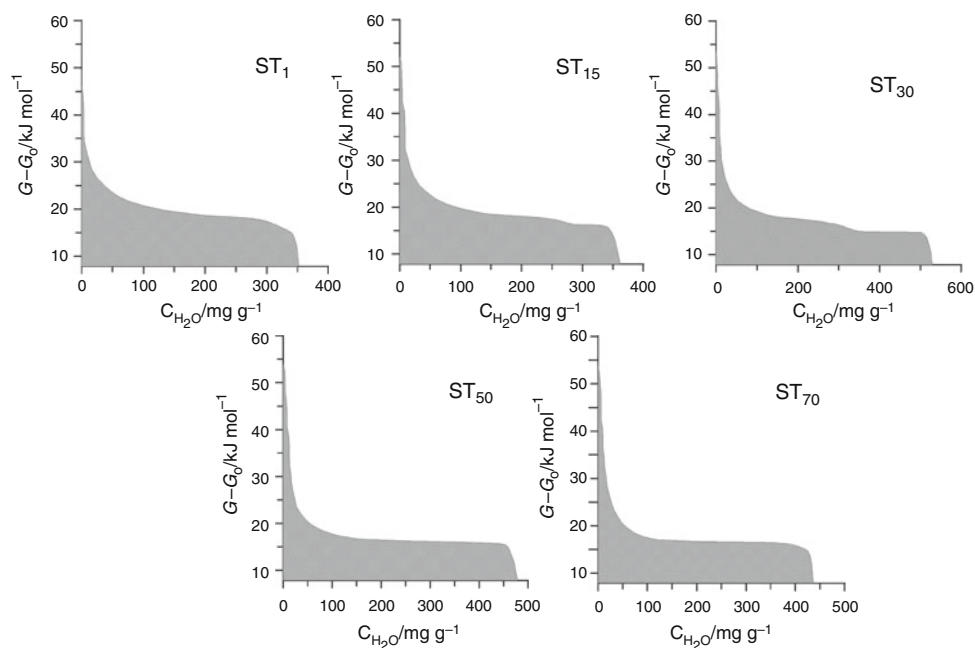


Table 2 Characterization of water adsorbed on the silica-titania adsorbents surface

Sample	$S_{\text{BET}}/\text{m}^2/\text{g}$	$C_{\text{H}_2\text{O}}^{\text{max}}/\text{mg}/\text{g}$	n	$\Delta G^{\text{s}}/\text{kJ}/\text{mol}$	$\Delta G^{\text{b}}/\text{kJ}/\text{mol}$	$\Delta G_{\Sigma}^{\text{s}}/\text{kJ}/\text{m}^2$	$\Delta G_{\Sigma}/\text{kJ}/\text{m}^2$
ST ₁	924	352.4	1.15	35.4	18.6	47	261
ST ₁₅	805	362.6	1.36	37.7	16.5	86	291
ST ₃₀	702	529.8	2.27	39.0	15.0	145	438
ST ₅₀	529	478.3	2.76	37.7	16.3	92	506
ST ₇₀	353	436.2	3.72	37.3	16.7	122	710

$C_{\text{H}_2\text{O}}^{\text{max}}$ is the maximal concentration of adsorbed water, n —the number of statistical adsorbed water layers, ΔG^{s} is a maximal value of changes in free energy for strongly adsorbed water, ΔG^{b} is the change in free energy of water during its evaporation from filled pores, $\Delta G_{\Sigma}^{\text{s}}$ is the surface free energy at the adsorbent/strongly bound water interface, ΔG_{Σ} is the total surface free energy at the adsorbent/water interface

narrower pores on the curve of pore volume distribution with respect to their average radius (Fig. 1b). These values are: $R = 1.04$ nm and 2.13 nm for ST₁₅, as well as $R = 1.14$ and 2.02 nm for ST₃₀ samples, respectively. The isotherms of the samples ST₅₀ and ST₇₀ are characterized by much lower adsorption in the range of low relative pressures and distinct hysteresis loops in that of high relative pressure. This gives a reflection in the course of the pore volume distribution functions on which we observe single peaks with the values of dominant radius R_{dom} equal to 1.89 and 2.43 nm for ST₅₀ and ST₇₀, respectively. The XRD analysis reveals that TiO₂ is in the form of anatase. The structural parameters of these adsorbents are shown in Table 1.

Figure 2 shows the experimental curves of water thermodesorption from the surface of the studied adsorbents as well as the DTG curves indicating the process rate depending on temperature. As can be seen larger the TiO₂ content is, the less complex is the thermodesorption of water from the pores. Three stages of this process are

observed for the adsorbents ST₁, ST₁₅, and ST₃₀ but only two for ST₅₀ and ST₇₀. Thermodesorption of weakly bound water from the ST₅₀ and ST₇₀ samples proceeds at lower temperatures and the inflection point occurs at 110 °C (Fig. 2). The other part of the water desorbs monotonically without visible stages pointing to a quick process. However, in the case of ST₁ and ST₁₅ the amount of weakly bound water is significantly smaller than that of strongly bound water desorbing at higher temperatures (above 110 °C). The intermediate properties with respect to the proportion of weakly and strongly bound water are exhibited by ST₃₀. Figure 2 shows the distinct differences in the course of vertical parts of the curves (desorption at different temperatures) as well as in the horizontal parts corresponding to differentiated sorption capacities of these adsorbents for water molecules. A good illustration is the summary picture presenting the curves of the water thermodesorption course in the temperature function (Fig. 3).

The shape of water thermodesorption curves correlates well with the courses of pore distribution functions with respect to their effective radius (Fig 1b). As can be seen the adsorbents ST₁ and ST₁₅ possessing mainly pores of narrow dimensions retain water molecules more strongly than the adsorbents ST₅₀ and ST₇₀ which exhibit porosity in the area of wider pores. However, the intermediate adsorbent ST₃₀ is characterized by the balanced proportion between narrow pores and wide pores as evidenced by the TG curve course (Fig. 3).

Two boundary phases exist on the adsorbent surface, when water is adsorbed on it, i.e., the adsorbent/water and

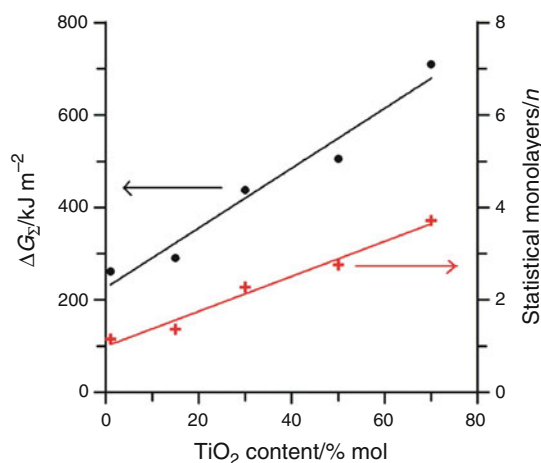


Fig. 5 The surface free energy at the adsorbent/water interface (ΔG_{Σ}) and the number of statistical water monolayers (n) in the dependences from the TiO₂ content

water/air interfaces. Thus, different reasons for a decrease in the Gibbs free energy of water at the adsorbent/water interface can be distinguished. These changes are caused by the strong adsorption of water molecules on the adsorbent surface centers (ΔG^s), capillary condensation in the pores (ΔG^{por}), and the presence of water/air interface (ΔG^{air}) [31]. When the Gibbs free energy of adsorbed water is equal to that of water in the gas phase (this process depends on the temperature and this is the condition for evaporation of adsorbed water), water begins to desorb from the surface when its Gibbs free energy becomes equal to that of water vapor at a given temperature (enabling possibility the phase transition). The thermodynamic function of the water vapor can be calculated using the equation:

$$\Delta G = G - G_0 = 0.197(T - T_0) \tag{2}$$

where T_0 is the standard temperature 293 K. On the basis of $\Delta m_{H_2O} = f(T)$ experimental data (Q-TG) the dependences of changes in the Gibbs free energy on the concentration of the adsorbed water were determined, $\Delta G = f(C_{H_2O})$.

Figure 4 presents the dependences of change of water free energy in the function of its concentration on the surface of the studied silica-titania adsorbents. The marked areas under these dependences were used to calculate the values of total surface free energy at the adsorbent/water interface (ΔG_{Σ}). However, the parts of these areas (corresponding to low concentrations of adsorbed water) were used to calculate the surface free energy at the adsorbent/strongly bound water interface (ΔG_{Σ}^s). The corresponding

Fig. 6 The dG/dM dependences as a function of statistical monolayers of water clusters for the silica-titania adsorbents

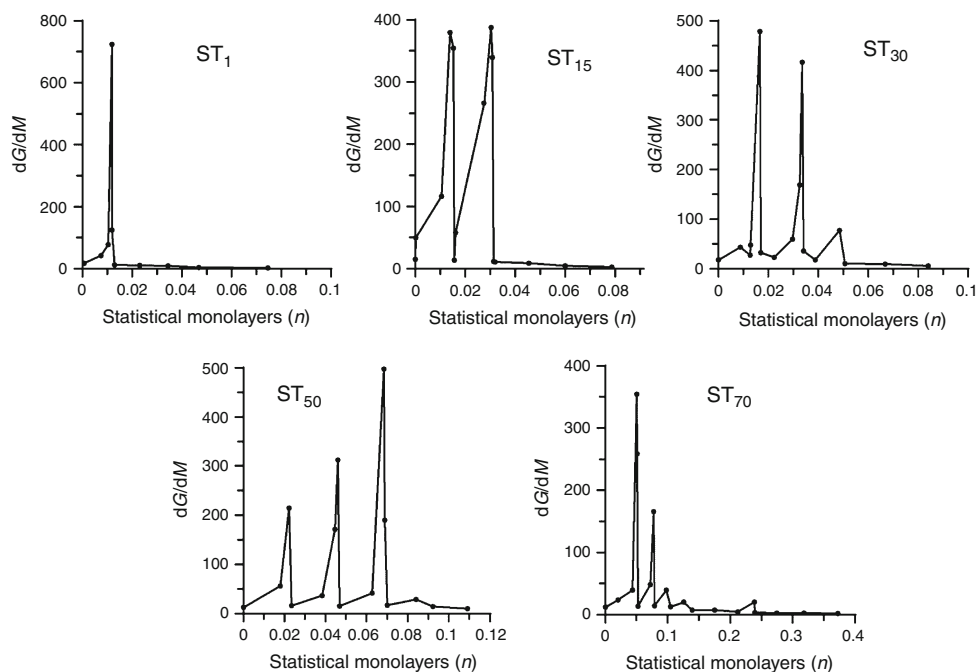


Fig. 7 The dependence of the effective radius of an evaporating drop on the concentration of adsorbed water

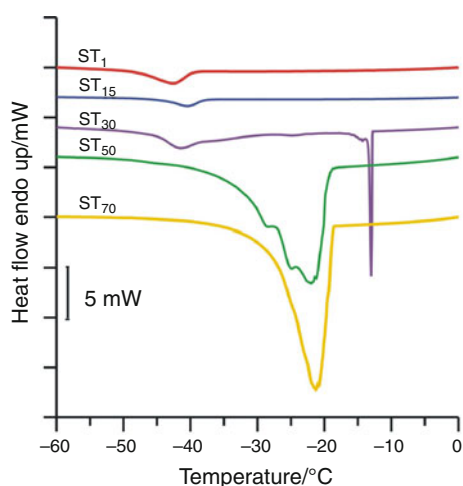
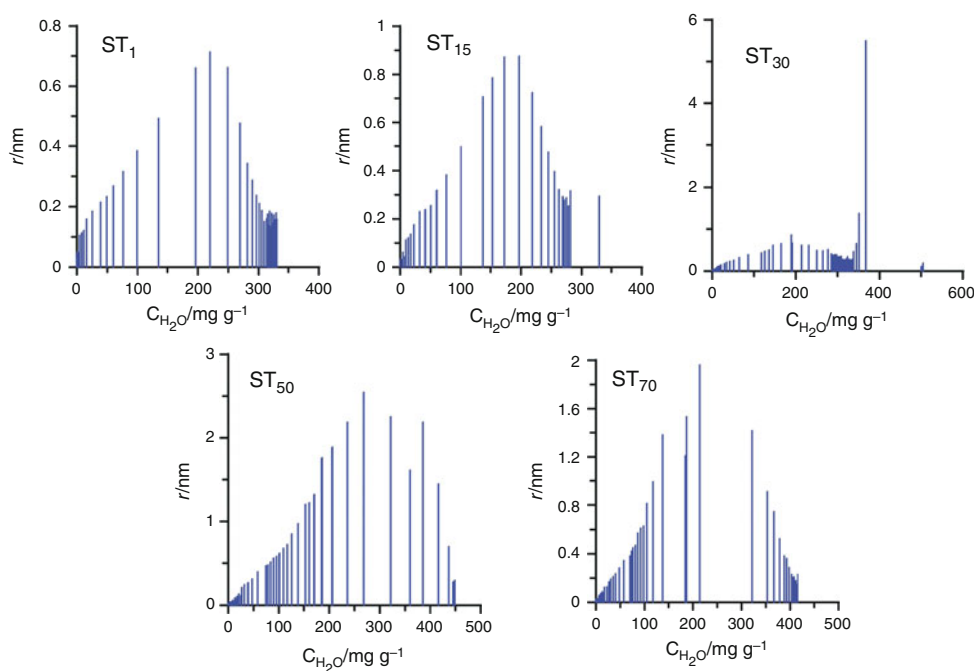


Fig. 8 DCS curves of water freezing in the pores of adsorbents containing the increasing amount of TiO₂

data are given in Table 2. As follows from the data in Table 2 the maximal concentration of the adsorbed water ($C_{\text{H}_2\text{O}}^{\text{max}}$) increases in the transition from the adsorbent ST₁ to the adsorbent ST₃₀ (with the increasing amount of TiO₂ in the adsorbent), and then decreases in the case of ST₅₀ and ST₇₀. This is connected with both the structure of complex porous adsorbents and their chemical composition. The above mentioned parameters are expressed in the values of the total surface free energy at the adsorbent/water interface (ΔG_{Σ}) and the surface free energy at the adsorbent/strongly bound water interface ($\Delta G_{\Sigma}^{\text{s}}$). As can be seen with the increasing content of TiO₂ in the studied adsorbents, the values of total surface free energy (ΔG_{Σ}) increase. In

the case of the parameter ($\Delta G_{\Sigma}^{\text{s}}$), a similar tendency can be observed except to the adsorbent ST₃₀ which is characterized by the highest value surface free energy at the adsorbent/strongly bound water interface (Fig. 5).

Figure 6 shows the dG/dM dependences as the function of statistical water monolayers, under the conditions of low coverage of adsorbent surface with water, where dG/dM is change in free energy of system with water mass changes. The value of the dG/dM derivative can be used as the analog of chemical potential in the description of isobaric process of thermodesorption. On the presented dependences one or two maxima can be observed, which indicate the formation of various types of water molecule clusters on the heterogeneous surface of the adsorbents under investigation. For the adsorbents of the smallest content of TiO₂ (ST₁ and ST₁₅ samples), there occurs a smaller number of maxima compared to other adsorbents (Fig. 6). Moreover, with the increasing amount of TiO₂ the observed maxima occur at thicker and thicker layers of adsorbed water, from 0.01 for ST₁ up to 0.25 for the ST₇₀ sample (Fig. 6).

Figure 7 shows the influence of the adsorbed water concentration on the effective radius of evaporated drops of water for the studied adsorbents. Comparing the obtained results with the data in Table 1, one can assume that the average radius of the evaporating drop has the size close to R_{ave} of the adsorbent. The numerical values of calculated radii should be treated with caution. The reason is that the basic assumption was the spherical shape of the drop and that the surface tension on the partition boundary is equal to that tension at the water/air interface. Actually a large

part of the drop outline is limited by the adsorbent surface. For this surface there should be chosen a different value of interface tension from that of surface tension.

The curves reflecting the energetic effects connected with water freezing inside the pores of investigated samples are presented in Fig. 8. Water contained in the pores of materials of strong adsorption properties is characterized by quite different physicochemical properties from those of volumetric water. In the case of the adsorbents possessing a well developed structure of micropores (ST₁, ST₁₅, and ST₃₀), the peaks of water freezing with the maximum at -42 °C are observed. This is caused by large impact of adsorbents surface (mainly micropores) on water molecules. In the case of the adsorbent with the intermediate content of TiO₂ (ST₃₀) there is observed the additional, distinctly formed peak of water freezing at -13 °C corresponding to that in the wider pores. This confirms the bimodal structure of this adsorbent. The peaks of water freezing for the ST₅₀ and ST₇₀ samples appear at about -22 °C, and their shapes indicate a large content of wide pores confirming the conclusion about their porous structure (Table 1; Fig. 1) and observations that water affected by the interactions with the surface of studied materials changes their physicochemical properties.

Conclusions

From the results of low-temperature adsorption–desorption of nitrogen measurements it was stated that the surface area of the obtained adsorbents varies from 924.1 m²/g (1% TiO₂) to 353.4 m²/g (70% TiO₂). The increase of the TiO₂ content in the silica-titania adsorbents results in the decrease of both its specific surface area and contribution of pores to its structure. The process of water thermodesorption from the surface of studied materials proceeds in two or three stages because of the pore distribution and TiO₂ content. With the increase of TiO₂ content in the studied adsorbents the values of total surface free energy (ΔG_{Σ}) increase. The largest value of the free surface energy at the adsorbent/strongly bound water interface is exhibited by the adsorbent of intermediate content (30%) of TiO₂. Different types of adsorbed water clusters occur with a larger extent of pores filling along with the increasing content of TiO₂ in the sample. Freezing temperature of water contained in the pores of studied materials depends largely on their porous structure. Water freezing in micropores of the tested materials proceed at about -42 °C, whereas, the water contained in wider pores freezes already at -22 °C. Due to the well developed porous structure, the water freezing process is a multi-stage one.

Acknowledgements This article was supported by the European Community FP7 under the Marie Curie International Research Staff Exchange Scheme (IRSES). Project No 230790.

Open Access This article is distributed under the terms of the Creative Commons Attribution Noncommercial License which permits any noncommercial use, distribution, and reproduction in any medium, provided the original author(s) and source are credited.

References

- Kresge CT, Leonowicz ME, Roth WJ, Vartuli JC, Beck JS. Ordered mesoporous molecular sieves synthesized by a liquid-crystal template mechanism. *Nature*. 1992;359:710–2.
- Blasco T, Corma A, Navarro MT, Pariente JP. Synthesis, characterization and catalytic activity of Ti-MCM-41 structures. *J Catal*. 1995;156:65–74.
- Corma A. From microporous to mesoporous molecular sieve materials and their use in catalysis. *Chem Rev*. 1997;97:2373–419.
- Orlov A, Zhai QZ, Klinowski J. Photocatalytic properties of the SBA-15 mesoporous silica molecular sieve modified with titanium. *J Mater Sci*. 2006;41:2187–93.
- Shen S, Deng Y, Zhu G, Mao D, Wang Y, Wu G, Li J, Liu X, Zhao D. Synthesis and characterization of Ti-SBA-16 ordered mesoporous silica composite. *J Mater Sci*. 2007;42:7057–61.
- Tanev PT, Chibwe M, Pinnavaia TJ. Titanium-containing mesoporous molecular sieves for catalytic oxidation of aromatic compounds. *Nature*. 1994;368:321–3.
- Koyano KA, Tatsumi T. Synthesis of titanium-containing MCM-41. *Microporous Mater*. 1997;10:259–71.
- Camprostrini R, Ischia M, Palmisano L. Pyrolysis study of sol-gel derived TiO₂ powders: part I. TiO₂-anatase prepared by reacting titanium(IV) isopropoxide with formic acid. *J Therm Anal Calorim*. 2003;71:997–1009.
- Balek V, Todorova N, Trapalis C, Štengl V, Večerníková E, Šubrt J, Malek Z, Kordas G. Thermal behavior of Fe₂O₃/TiO₂ mesoporous gels. *J Therm Anal Calorim*. 2005;80:503–9.
- Balek V, Šubrt J, Bountseva IM, Irie H, Hashimoto K. Emanation thermal analysis study of N-doped titania photoactive powders. *J Therm Anal Calorim*. 2008;92:161–7.
- Mousa MA, Farid T, Omran ZA, Allah EMD. Physicochemical studies on the TiO₂-silica gel system. *J Therm Anal Calorim*. 1994;42:1103–12.
- Corma A, Kan Q, Rey F. Synthesis of Si and Ti-Si-MCM-48 mesoporous materials with controlled pore sizes in the absence of polar organic additives and alkali metal ions. *Chem Commun*. 1998;579–580.
- Sayari A, Liu P. Non-silica periodic mesostructured materials: recent progress. *Microporous Mater*. 1997;12:149–77.
- Yanishpolskii VV, Pavlenko AN, Tertykh VA, Il'in VG, Leboda R, Skubiszewska-Zięba J. Mesoporous titanium-containing silicas. Synthesis and geometrical characteristics. *J Therm Anal Calorim*. 2000;62:569–73.
- Tasbihi M, Stangar UL, Skapin AS, Ristic A, Kaucic V, Tusar NN. Titanium-containing mesoporous silica powders: structural properties and photocatalytic activity towards isopropanol degradation. *J Photochem Photobiol A*. 2005;169:101–7.
- Yin H, Wada Y, Kitamura T, Kambe S, Murasawa S, Mori H, Sakata T, Yanagida S. Hydrothermal synthesis of nanosized anatase and rutile TiO₂ using amorphous phase TiO₂. *J Mater Chem*. 2001;11:1694–703.
- Mihai GD, Meynen V, Beyers E, Mertens M, Bilba N, Cool P, Vansant EF. Synthesis, structural characterization and

- photocatalytic activity of Ti-MCM-41 mesoporous molecular sieves. *J Porous Mater.* 2009;16:109–18.
18. Luan Z, Meloni PA, Czernuszewicz RS, Kevan L. Raman spectroscopy of vanadium oxide species immobilized at surface titanium centers of mesoporous titanosilicate TiMCM-41 molecular sieves. *J Phys Chem B.* 1997;101:9046–51.
 19. Bourlinos AB, Karakassides MA, Petridis D. Synthesis and characterization of iron-containing MCM-41 porous silica by the exchange method of the template. *J Phys Chem B.* 2000;104:4375–80.
 20. Hagen A, Schueler K, Roessner F. The performance of the Ti-MCM-41 in aqueous media and after mechanical treatment studied by in situ xanes, uv/vis and test reactions. *Microporous Mesoporous Mat.* 2002;51:23–33.
 21. Kornatowski J, Wichterlova B, Jitkovsky J, Loffler E, Pilz W. Spectroscopic studies of vanadium-substituted zeolitic silicates of MFI topology. *J Chem Soc Faraday Trans.* 1996;92:1067–78.
 22. Crişan M, Brăileanu A, Crişan D, Răileanu M, Drăgan N, Mardare D, Teodorescu V, Ianculescu A, Bîrjega R, Dumitru M. Thermal behaviour study of some sol-gel TiO₂ based materials. *J Therm Anal Calorim.* 2008;92:7–13.
 23. Nishide T, Tanaka T, Yabe T. Temperature programmed desorption analysis of sol-gel-derived titanium films: design of a sol preparation procedure. *J Therm Anal Calorim.* 2007;90:373–8.
 24. Ingo GM, Riccucci C, Bultrini G, Dirè S, Chiozzini G. Thermal and microchemical characterisation of sol-gel SiO₂, TiO₂ and xSiO₂-(1-x)TiO₂ ceramic materials. *J Therm Anal Calorim.* 2001;66:37–46.
 25. Cides da Silva LC, Araujo GLB, Segismundo NR, Moscardini EF, Mercuri LP, Cosentino IC, Fantini MCA, Matos JR. DSC estimation of structural and textural parameters of SBA-15 silica using water probe. *J Therm Anal Calorim.* 2009;97:701–4.
 26. Marinescu C, Sofronia A, Rusti C, Piticescu R, Badilita V, Vasile E, Baies R, Tanasescu S. DSC investigation of nanocrystalline TiO₂ powder. *J Therm Anal Calorim.* 2011;103:49–57.
 27. Wan Q, Ramsey Ch, Baran G. Thermal pretreatment of silica composite filler materials. *J Therm Anal Calorim.* 2010;99:237–43.
 28. Gregg SJ, Sing KSW. Adsorption, surface area and porosity. London: Academic Press; 1982.
 29. Barrett EP, Joyner LG, Halenda PP. The determination of pore volumes and area distributions in porous substances. *J Am Chem Soc.* 1951;73:373–80.
 30. Turov VV, Lebeda R, Skubiszewska-Zięba J, Charmas B. Application of quasi-isothermal thermogravimetry for estimation of some properties of hydration layers in mesoporous adsorbents. *Colloid Surf A.* 2001;181:1–9.
 31. Skubiszewska-Zięba J. Structural and energetic properties of carbosils hydrothermally treated in the autoclave or the microwave reactor. *Adsorption.* 2008;14:695–709.